

The BATSE-*Swift* luminosity and redshift distributions of short-duration GRBs

D. Guetta¹ and T. Piran²

¹ Osservatorio astronomico of Rome, v. Frascati 33, 00040 Monte Porzio Catone, Italy
e-mail: dafne@arcetri.astro.it

² Racah Institute for Physics, The Hebrew University, Jerusalem 91904, Israel

Received 9 November 2005 / Accepted 9 March 2006

ABSTRACT

We compare the luminosity function and rate inferred from the BATSE peak flux distribution of short hard bursts (SHBs) with the redshift and luminosity distributions of SHBs observed by *Swift*/HETE II. While the *Swift*/HETE II SHB sample is incompatible with the SHB population that follows the star formation rate, it is compatible with an SHB rate that reflects a distribution of delay times after the SFR. This would be the case if SHBs were associated with binary neutron star mergers. The available data allows, however, different interpretations. For example, a population whose rate is independent of the redshift fits the data very well. The implied SHB rates that we find range from ~ 8 to $\sim 30 h_{70}^3 \text{ Gpc}^{-3} \text{ yr}^{-1}$. This rate, which is comparable to the rate of neutron star mergers estimated from statistics of binary pulsars, is a much higher rate than what was previously estimated. We stress that our analysis, which is based on *observed* SHBs, is limited to bursts with luminosities above 10^{49} erg/s . Weaker bursts may exist, but if so they are hardly detected by BATSE of *Swift*, so their rate is very weakly constrained by current observations.

Key words. cosmology: observations – gamma rays: bursts – gravitational waves

1. Introduction

It has been known since the early nineties that gamma-ray bursts (GRBs) are divided into two subgroups of long and short according to their duration: $T_{90} \lesssim 2 \text{ s}$ (Kouveliotou et al. 1993). Short bursts are also harder than long ones (Dezalay et al. 1996; Kouveliotou et al. 1996; Qin et al. 2000), so they are denoted as short hard bursts (SHBs). Our understanding of long bursts and of their association with stellar collapse followed from the discovery in 1997 of GRB afterglow and the subsequent identification of host galaxies, redshift measurements, and even detection of associated supernovae. However, until recently no afterglow has been detected from any short burst, so they remained as mysterious as ever.

This situation has changed with the detection of X-ray afterglow from several short bursts by *Swift* (Gehrels et al. 2005; Romano et al. 2005) and by HETE II (Villasenor et al. 2005). In some cases, optical (Covino et al. 2005; Fox et al. 2005; Bloom et al. 2006; Price et al. 2005; Jensen et al. 2005; Hjorth et al. 2005; Castro-Tiraldó et al. 2005; Gal-Yam et al. 2005b; Cobb et al. 2005; Wiersema et al. 2005) and radio (Cameron & Frail 2005; Berger 2005) afterglow was detected as well. This has led to the identification of host galaxies and to redshift measurements. While the current sample is very small, several features have emerged. First, unlike long GRBs that take place in galaxies with young stellar populations, SHBs also take place in elliptical galaxies in which the stellar population is older. In this they behave like type Ia supernovae. The redshift and peak (isotropic equivalent) luminosity distributions of the five short bursts (see Table 1) indicate that the observed SHB population is significantly nearer than the observed long-burst population. This feature was expected (Piran 1994; Katz & Canel 1996;

Tavani 1998; Guetta & Piran 2005, denoted hereafter GP05), as the $\langle V/V_{\text{max}} \rangle = 0.39 \pm 0.02$ of the BATSE short-burst population was significantly larger (and closer to the Euclidian value of 0.5) than the one of long bursts ($\langle V/V_{\text{max}} \rangle = 0.29 \pm 0.01$, Guetta et al. 2004, denoted hereafter as GPW).

Recently GP05 have estimated the luminosity function and formation rate of SHBs from the BATSE peak flux distribution. These two quantities are fundamental to understanding the nature of these objects. The observed flux distribution is a convolution of these two unknown functions, so it is impossible to determine both functions without additional information. Already in 1995 Cohen & Piran (1995) showed that the observed BATSE flux distribution can be fitted with very different luminosity functions, depending on the choice of the GRB rate. GP05 show that the distribution is compatible with either a population of sources that follow the SFR (like long bursts) or with a population that lags behind the SFR (Piran 1992; Ando 2004). There are several reasons to expect (see e.g. Narayan et al. 2001) that SHBs may be linked to binary neutron star mergers (Eichler et al. 1989). In such a case the SHB rate is given by the convolution of the star formation rate with the distribution $P_m(\tau)$ of the merging time delays τ in the binary system. These delays reflect the time it takes for the system to merge due to emission of gravitational radiation.

As BATSE is less sensitive to short bursts than to long ones (Mao et al. 1994), even an *intrinsic* SHB distribution that follows the SFR gives rise to an *observed* distribution that is nearer to us. Still a delayed SFR distribution (that is *intrinsically* nearer) gives rise to even nearer *observed* distribution (GP05). Therefore the recent *observed* redshift distribution of SHBs favors the delayed model and hence the merger scenario. Still the question was posed as to whether the predicted (GP05) *observed*

Table 1. The current *Swift*/HETE II sample of SHBs with known redshift. $L_{\gamma,iso,51} = L_{\gamma,iso}/10^{51}$ erg/s.

GRB	050509b	050709	050724	050813	051221
z	0.22	0.16	0.257	0.7 or 1.80	0.5465
$L_{\gamma,iso,51}$	0.14	1.1	0.17	1.9	3

distribution is consistent with the current sample. Gal Yam et al. (2005a) suggest that the distributions are inconsistent, so the suggested delayed SFR model is ruled out. We re-examine the situation here and show that, while a delayed distribution with “maximal likelihood” parameters are indeed ruled out, a delayed distribution with parameters within 1σ of the best-fit parameters cannot be ruled out with the current SHB redshift distribution. We discuss the implications of this result to GRBs, to binary Neutron star mergers, and to the detection of gravitational radiation from such mergers.

2. The luminosity function of the BATSE SHB sample

Our data set and methodology follow GP05. We consider all the SHBs that were detected while the BATSE onboard trigger (Paciesas et al. 1999) was set for 5.5σ over background in at least two detectors in the energy range 50–300 keV. These constitute a group of 194 bursts. Following a physical model, we assumed a rate of bursts. We then search for a best fit luminosity function. Using this luminosity function we calculate the expected distribution of *observed* redshifts and compare it with the present data.

We consider the following cosmological rates:

- (i) A rate that follows the SFR. We do not expect that this reflects the rate of SHBs but we include this case for comparison;
- (ii) A rate that follows the NS-NS merger rate. This rate depends on the formation rate of NS binaries, which one can safely assume follow the SFR, and on the distribution of merging time delays. This, in turn, depends on the distribution of initial orbital separation a between the two stars ($\tau \propto a^4$) and on the distribution of initial eccentricities. Both are unknown. From the coalescence time distribution of six double neutron star binaries (Champion et al. 2004), it seems that $P(\log(\tau))d\log(\tau) \sim \text{const.}$, implying $P_m(\tau) \propto 1/\tau$, in agreement with the suggestion by Piran (1992). Therefore our best guess scenario is an SBH rate that follows the SFR with a logarithmic time delay distribution. In this case the normalization of $P(\tau)$ is such that $P(\tau) \neq 0$ only for $20 \text{ Myr} < \tau < \text{age of the universe}$. Obviously delays longer than the age of the universe do not add events;
- (iii) a rate that follows the SFR with a delay distribution $P(\tau)d\tau \sim \text{const.}$ In this case the normalization of $P(\tau)$ is such that $P(\tau) \neq 0$ only for $0 < \tau < \text{age of the universe}$;
- (iv) a constant rate (which is independent of redshifts.).

For the SFR needed in distributions (i–iii), we employ the SF2 model of Porciani & Madau (2001):

$$R_{\text{SF2}}(z) = \rho_0 \frac{23 \exp(3.4z)[\Omega_M(1+z)^3 + \Omega_k(1+z)^2 + \Omega_\Lambda]^{1/2}}{(\exp(3.4z) + 22)(1+z)^{3/2}}, \quad (1)$$

Table 2. Best fit parameters $\text{Rate}(z=0)$, L^* , α , β and their 1σ confidence levels for models (i)–(iv).

	$\text{Rate}(z=0)$ $\text{Gpc}^{-3} \text{yr}^{-1}$	L^* 10^{51}erg/s	α	β	χ^2	KS test ($z=0.7$)	KS test ($z=1.8$)
i	$0.11^{+0.07}_{-0.04}$	$4.6^{+2.2}_{-2.2}$	$0.5^{+0.4}_{-0.4}$	$1.5^{+0.7}_{-0.5}$	25.5	<0.01	<0.01
ii	$0.6^{+8.4}_{-0.3}$	$2^{+2}_{-1.9}$	$0.6^{+0.4}_{-0.4}$	2 ± 1	24.9	0.05	0.06
ii $_\sigma$	10^{+8}_{-5}	0.1	$0.6^{+0.2}_{-0.4}$	1 ± 0.5	26	0.22	0.25
iii	30^{+50}_{-20}	$0.2^{+0.5}_{-0.195}$	$0.6^{+0.3}_{-0.5}$	$1.5^{+2}_{-0.5}$	24.7	0.91	0.91
iv	8^{+40}_{-4}	$0.7^{+0.8}_{-0.6}$	$0.6^{+0.4}_{-0.5}$	$2^{+1}_{-0.7}$	24.5	0.41	0.41

where ρ_0 is the present GRB rate and $\Omega_{M,\Lambda,k}$ are the present cosmological parameters. In models (ii) and (iii) the rate of SHBs is given by:

$$R_{\text{SHB}}(z) = C_1 \int_0^{t(z)} d\tau R_{\text{SF2}}(t-\tau) P_m(\tau), \quad (2)$$

where $P_m(\tau)$ is the distribution of the merging time delays τ and C_1 a normalization constant.

Following Schmidt (2001), GPW, and GP05, we consider a broken power-law peak luminosity function with lower and upper limits, $1/\Delta_1$ and Δ_2 , respectively:

$$\Phi_0(L)d\log L = C_0 d\log L \begin{cases} (L/L^*)^{-\alpha} & L^*/\Delta_1 < L < L^* \\ (L/L^*)^{-\beta} & L^* < L < \Delta_2 L^* \end{cases}, \quad (3)$$

where C_0 is a normalization constant. This is the “isotropic-equivalent” luminosity function; i.e. it does not include a correction factor due to the fact that GRBs are beamed. In our calculations we approximate, following Schmidt (2001), the typical effective spectral index in the observed range of 20 or 50 keV to 300 keV as -1.1 ($N(E) \propto E^{-1.1}$).

Following GP05 we use $\Delta_{1,2} = (30, 100)$. Both values are chosen in such a way that, even if there are bursts less luminous than L^*/Δ_1 or more luminous than $\Delta_2 L^*$, they will only be very few (less than about 1%) of the *observed* bursts outside the range $(L^*/\Delta_1, L^*\Delta_2)$. Bursts above $L^*\Delta_2$ are very bright and are detected to very large distances. However, there are very few bursts above $L^*\Delta_2$. Increasing Δ_2 does not add a significant number of bursts (observed or not) and this does not change the results. In particular it does not change the overall rate and Δ_1 is subtler. The luminosity function increases rapidly with decreasing luminosity, so that a decrease in Δ_1 will have a strong effect on the overall rate of short GRBs. However, it is important to realize that most of the bursts below L^*/Δ_1 are undetectable by existing detectors, unless they are extremely nearby, even if the luminosity function continues all the way to zero. This will increase the overall rate of the bursts enormously (which will in fact diverge in this extreme example); however, most of these additional weak bursts will be undetected, and the total number of detected bursts will not increase. For example, in our ii $_\sigma$ model only 1% of the BATSE detected bursts would have, in this extreme case, a luminosity below L^*/Δ_1 . Clearly, the BATSE data does not constrain this part of the luminosity-phase space so the question what is the number of such weak bursts remains open, at least as far as the observed flux distribution is concerned.

Comparing the predicted distribution with the one observed by BATSE we use a minimum χ^2 method, to obtain the best fit parameters of each model and their standard deviation (see Table 2). In order to assign an χ^2 value we divided the 193 bursts

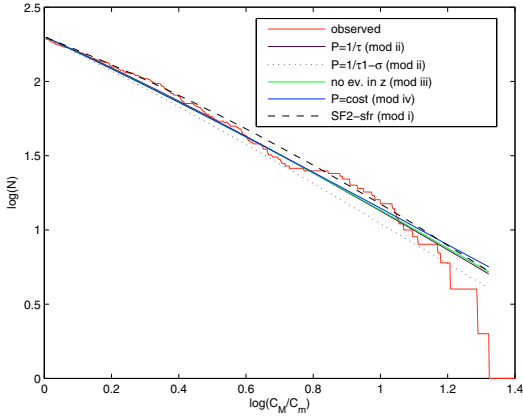


Fig. 1. The predicted $\log N - \log(P/P_{\text{lim}})$ distribution vs. the observed $\log N - \log(C_M/C_m)$ taken from the BATSE catalog for the best-fit values of α , β and L^* with models (i)–(iv). C_M is the count rate in the second brightest illuminated detector, and C_m the minimum detectable rate. Also shown is the curve where the L^* value is lower by 1σ than the best-fit one for case (ii), which we call model (ii $_{\sigma}$).

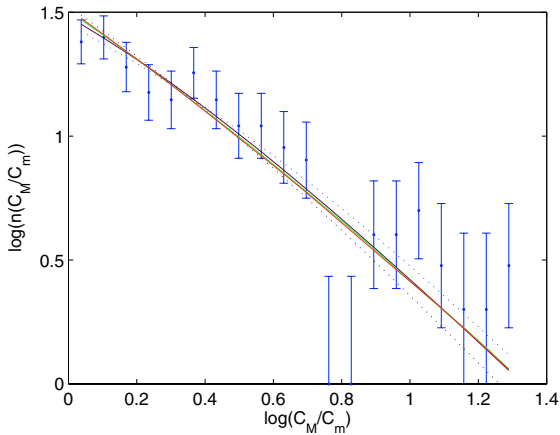


Fig. 2. The predicted differential distribution, $n(P/P_{\text{lim}})$, vs. the observed $n(C_M/C_m)$ taken from the BATSE catalog for the best fit values of α , β , and L^* with models (i)–(iv) and (ii $_{\sigma}$).

in the BATSE catalog into 20 bins of equal size according to their value of P , the peak photon flux. Since the overall normalization is an additional free parameter, the number of degree of freedom is $20 - 4 = 16$. The results are presented in Table 2 and in Figs. 1 and 2, which depict comparisons between the predicted integrated and differential distributions and the observed one (using the best fit parameters for the luminosity function). In Table 2 we report the best fit parameters: Rate($z = 0$), L^* , α , β and their 1σ confidence levels for models (i)–(iv). Also shown are the goodness of the fit and the KS probability that the five bursts with a known redshift arise from this distribution. We show two results for KS tests one with GRB 050813 at $z = 0.7$ and the other at $z = 1.8$. For each parameter the 1σ range is marginalized over the variation in all other parameters. The case ii $_{\sigma}$ corresponds to case ii with an L^* value lower by 1σ than the best fit one, and we show also this model in Fig. 1. Other parameters have been best fitted for this fixed number. Below this value of L^* the quality of the fit decreases very quickly. The possibility of decreasing L^* by a factor 10 and still getting a reasonable fit is a crucial point of our analysis. In fact this is the key to making the BATSE results compatible with the low z distribution observed by *Swift* as we show in the next section. This is also the reason why the current estimates give a much higher rate.

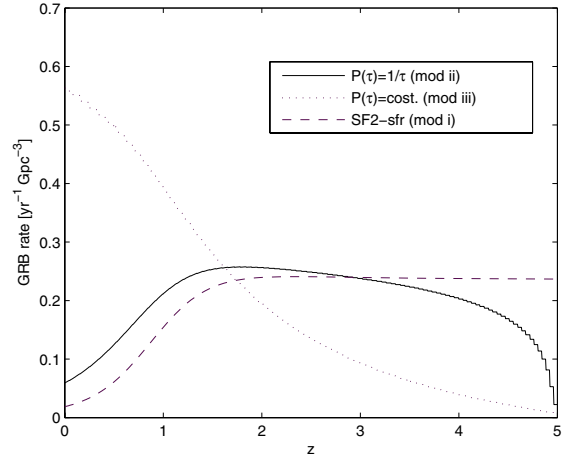


Fig. 3. The rate of SHBs for the different models (i)–(iii). Model (iv) would be represented by a constant line. Note that the event rate of models ii and ii $_{\sigma}$ is the same as the difference between the two models is in the luminosity function and not in the event rate.

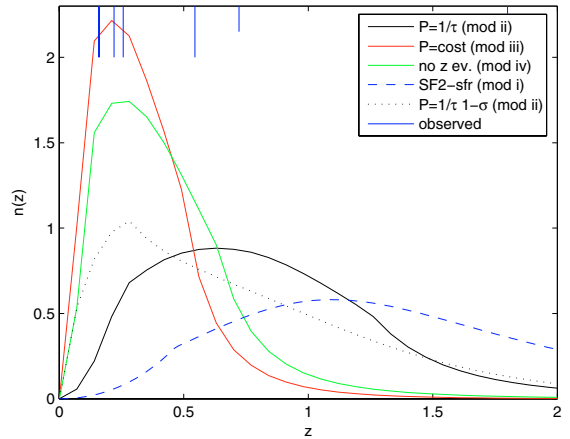


Fig. 4. The expected *observed* differential redshift distributions of SHBs for models (i)–(iv) and (ii $_{\sigma}$). The known redshifts of five SHBs are shown as vertical lines. The two small vertical lines corresponds to $z = 0.7$ and $z = 1.8$.

3. Comparison with the current *Swift*-HETE II SHB sample

We can now derive the expected redshift distribution of the observed bursts' population in the different model:

$$N(z) = \frac{R_{\text{GRB}}(z)}{1+z} \frac{dV(z)}{dz} \int_{L_{\text{min}}(P_{\text{lim}},z)}^{L_{\text{max}}} \Phi_0(L) d\log L, \quad (4)$$

where $L_{\text{max}} = \Delta_2 L^* = 100L^*$, and $L_{\text{min}}(P_{\text{lim}},z)$ is the luminosity corresponding to minimum peak flux P_{lim} for a burst at redshift z . This minimal peak flux corresponds to the detector's threshold. For BATSE, $P_{\text{lim}} \sim 1$ ph/cm²/s for short bursts. The triggering algorithm for *Swift*, is rather complicated but it can be approximated by a comparable minimal rate: $P_{\text{lim}}(\text{Swift}) \sim 1$ ph/cm²/s.

Figure 3 depicts the SHB rate density as a function of redshift for the different τ distributions and compare the results with a distribution that follows the SFR (SF2). As expected, the time delay increases the number of short bursts at low redshift. In particular there is a dramatic increase if $P(\tau)d\tau \sim \text{const}$. Figures 4 and 5 depict the expected *observed* (differential and integrated, respectively) redshift distributions of SHBs in the different models.

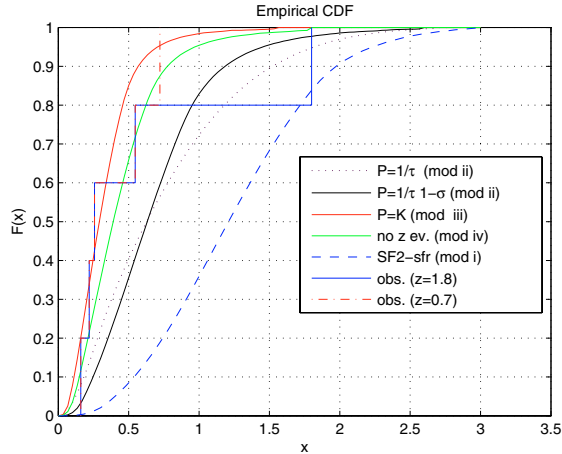


Fig. 5. A comparison between the expected integrated *observed* redshift distributions of SHBs for models (i)–(iv) and (ii_σ) and the distribution of known redshifts of SHBs.

As expected, a distribution that follows the SFR, case (i), is ruled out by a KS test with the current five bursts (the p -value is smaller than 1%). This is not surprising as other indications, such as the association of some SHBs with elliptical galaxies, suggest that SHBs are not associated with young stellar populations.

A distribution that follows the SFR with a constant logarithmic delay distribution, case (ii), is more interesting. A priori, this was our favorite distribution as a logarithmic distribution of separations between the two members of a NS-binary (or a BH-NS binary) would lead to a logarithmic distribution of time delays (Piran 1992). At first glance, this distribution is marginally consistent with the data. A KS test suggests that the probability of the observed data arising from this distribution is ~ 5 –6% (see also Gal-Yam 2005a). The observed bursts are nearer (lower redshift) than expected from this distribution. It is interesting that the addition of a fifth burst (GRB 051221A) that was detected after a first version of this paper was submitted improved the KS test value of this model slightly. Additionally, if we use the Rowan-Robinson SFR (see GP05), rather than the SF2 of Porciani-Madau, the KS test for this model is 10% (for either $z = 0.7$ or $z = 1.8$).

While it is possible that the real distribution of time delays is not logarithmically constant, there are several other possible explanations for this result. First turning to the data, we realize that selection effects that determine which SHB is detected and *localized* with sufficient accuracy to allow redshift determination are not clear. It is possible that we are dealing with small number statistics. It is also possible that the afterglows of these five localized bursts are brighter than the afterglow of typical, more distant bursts, and that this has influenced the sample. A second possibility is that the current data is a good sample of the SHB distribution but that the “best fit” parameters estimated using the BATSE SHB population are slightly offset, due to a statistical fluctuation. For example, we have considered a distribution in case (ii_σ) whose typical luminosity, L^* , is one σ away from the maximal likelihood value. This distribution, which is consistent with the BATSE SHB sample is not ruled out by the current sample of SHBs with a known redshift. The p value of the KS test is 0.1.

As an example of the flexibility of the data, we considered two other time delay distributions: case (iii), in which the time delay distribution is uniform, and case (iv), in which the overall SHB rate is constant in z . Both cases are compatible with the

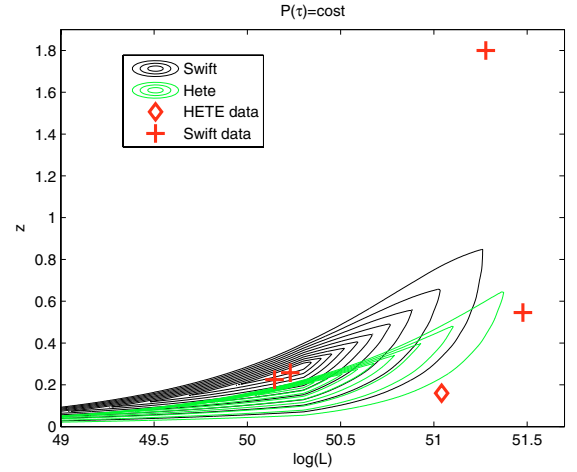


Fig. 6. The two-dimensional probability distribution of expected redshift and luminosity for model (iii) considering the sensitivity of *Swift* (black) and HETE (green). Contour lines are 0.9, 0.8, ..., 0.1 of the maximum. Also marked are the five SHBs with a known redshift.

BATSE SHB distribution and with the sample of SHBs with a known redshift (the KS p values are 0.8 and 0.4, respectively). This result is not surprising. The BATSE peak flux distribution depends on two unknown functions, the rate and the luminosity function. There is enough freedom to choose one function (the rate) and fit for the other. The sample of SHBs with known redshifts peaks at a rather low redshift, and both distributions considered above push the intrinsic SHB rate to lower redshifts (as compared to the SFR).

In all cases that are compatible with the five bursts with a known redshift, the *intrinsic* SHB rate is pushed towards lower redshifts and the present rates (needed to fit the observed BATSE rate) are higher by almost two orders of magnitude than those earlier estimates assuming that SHBs follow the SFR or that they follow it with a logarithmic delay (with the best fit parameters). These rates are ~ 30 , ~ 8 , and $\sim 10 h_0^3 \text{ Gpc}^{-3} \text{ yr}^{-1}$ for cases (iii), (iv), and (ii_σ), respectively. The corresponding “typical” luminosities, L^* , range from 0.1 to $0.7 \times 10^{51} \text{ erg/s}$.

We also considered delay distributions that are peaked at a given delay (such as a log-normal distribution), but we do not present them here for lack of space. A narrow distribution results simply in an SFR with a fixed delay. If the typical delay is long enough, it will push the intrinsic SHB rate to redshift that is low enough. However, the current distribution of the merging time of binary pulsars (Champion et al. 2004; GP05) indicates that the distribution is wide. A wide distribution, such as a distribution with a typical delay of 10^9 years and a spread of two decades results in an overall rate that is very similar to one resulting from a logarithmic distribution.

Before turning to the implications of these results we should, however, re-examine the fit of the data sets to the model. One way to do so is to compare the expected 2 dimensional distribution of bursts in the $(z, \log(L))$ plane with the observed *Swift*/HETE II bursts. Figure 6 depicts such a comparison for our best model (iii). Since GRB 050709 was determined by HETE, we have reproduced the contours considering both the *Swift* and HETE sensitivities. While two of the bursts are just where we expect them to be, the others are in low probability regions. Similar behavior arises for the other models as well. One can apply a sophisticated 2D KS test (Bahcall et al. 1987) to estimate the probability that the data and the models are consistent, but given the small number of bursts we feel that this is not necessary at this

stage. It is sufficient to say that an eye, inspection suggests an inconsistency between all models and the *Swift*/HETE II data.

There are several ways to explain this apparent inconsistency. Once more we can turn to small number statistics and argue that it is difficult to make far reaching conclusions from such a few bursts. However, it is also possible that the data indicates a real discrepancy between the BATSE data (on which the models are based) and the *Swift*/HETE II data (to which the models are compared). This is not surprising as the triggering algorithm, as well as the energy bands in which different bursts are observed in these two experiments, are drastically different. It is possible, for example, that we are underestimating the limiting peak flux needed for detection by *Swift*. An increase in the estimated threshold of *Swift* would have improved the fit. Another issue that could influence the comparison is the existence of selection effects that influence the detectability of the redshift of SHBs. Such selection effects could, of course, influence the sample of observed bursts with known redshift.

It is also possible that these results indicate that there is something new in the data. A glance at Fig. 2 (the differential distribution of observed fluxes of short BATSE bursts) indicates a deep at an intermediate-high peak flux level, at $P = 6$ photons/cm²/s, about 6 times the minimal detectable flux. This is a flux level in which there is no observational reason why BATSE should have missed bursts. Still, a marginally significant deep is there. Is it possible that this deep reflects a real phenomenon and that there are two populations of SHBs? That is one that gives rise to the highest fluxes (at a level of ~ 10 photons/cm²/s) and another that gives rise to the low flux ones. A related conclusion has been reached recently using independent reasoning by Tanvir et al. (2005).

4. Conclusions and implications

We repeated the analysis of fitting the BATSE SHB data to a model of the luminosities and rate distributions. We stress that the fit to the BATSE data is similar to the one presented in GP05. Our best-fit logarithmic distribution model is similar to the best-fit logarithmic model presented in GP05. Our results and, in particular, the estimated rates seem very different from those obtained in GP05, but a glance at Table 2 shows that the 1σ spread in the rate is indeed very large! A main new ingredient of this work is the fact that we consider several other models. All fit the BATSE data equally well. We confirm our earlier finding that the BATSE data allows a lot of flexibility in the combination of the rates and luminosities. In GP05 we have shown that the BATSE data is compatible with a distribution that follows the SFR and one that has a logarithmic time lag. Here we also consider additional distributions.

A second new ingredient in this work is the comparison of the best fit models to the small sample of five *Swift*/HETE II SHBs. The *Swift*/HETE II data gives a new constraint. This constraint favors a population of SHBs with a lower intrinsic luminosity and hence a nearer *observed* redshift distribution. If this interpretation is correct, it implies a significantly higher local SHB rate – a factor 50 or so higher than earlier estimates. We stress again that this new result was within the 1σ error of the model presented in GP05. The difference between the conclusions in GP05 and the conclusions of this paper arises because of the new observations of *Swift* that show that the SHBs are nearer than what was expected before. This can arise due to one of the following possibilities: 1) the logarithmic time delay model is wrong; 2) the model is right but the best fit parameters are 1σ away from the real ones or that the small *Swift* sample is

misleading; 3) the *Swift* SHB set have significantly different selection effects than the BATSE SHB set. Such a situation would arise if there are two populations of short bursts that are detected at different combinations by *Swift* and by BATSE.

Provided that the basic model is correct and we are not being misled by statistical (small numbers), observational (selection effects and threshold estimates) or intrinsic (two SHB population) factors, we can proceed comparing the inferred SHB rate with the observationally inferred rate of NS-NS mergers in our galaxy (Phinney 1992; Narayan et al. 1992). This rate was recently re-evaluated with the discovery of PSR J1829+2456 being rather large at 80^{+200}_{-66} /Myr, although the estimate contains a fair amount of uncertainty (Kalogera et al. 2004). If we assume that this rate is typical and that the number density of galaxies is $\sim 10^{-2}$ /Mpc³, we find a merger rate of 800^{+2000}_{-660} /Gpc³/yr. Recently Berger et al. (2005) have derived a beaming factor of 30–50 for short bursts. This rate implies a total merger rate of ~ 240 – 1500 /Gpc³/yr for the three cases (iii), (iv), and (ii $_{\sigma}$). The agreement between the completely different estimates is surprising and could be completely coincidental, as both estimates are based on very few events.

If correct, these estimates are excellent news for gravitational radiation searches, for which neutron star mergers are prime targets. They imply that the recently updated high merger rate, depends mostly on one object, PSR J0737-3039, is valid. These estimates which imply one merger event within ~ 70 Mpc per year and one merger accompanied with an SHB within ~ 230 Mpc. These ranges are almost within the capability of LIGO I, and certainly within the capability of LIGO II. In these estimates we considered a luminosity function with a sharp cutoff at a few $\times 10^{49}$ erg/s. However Δ_1 is unconstrained in our calculations and it is possible that there are many more mergers. Bursts with lower peak luminosity are practically undetectable by current detectors. Such bursts, if they exist, constitute a very small fraction (a few percent at most) of the *observed* burst population. Therefore, using the current GRB data, we cannot rule out or verify their existence. From this point of view one should consider our estimates of the rates of SHBs and hence the rate of neutron star mergers as lower limits. It is possible that the actual rate is much higher. If true this could be tested by LIGO I and II within the next few years.

Acknowledgements. This research was supported by the US-Israel BSF and by the Schwarzmann university chair (TP).

References

- Ando, S. 2004, JCAP, 06, 007
- Bahcall, J. N., Spergel, D. N., Piran, T., & Press, W. H. 1987, Nature, 327, 682
- Berger, E., Price, P. A., Cenko, S. B., et al. 2005, Nature, 438, 988
- Bloom, J. S., Prochaska, J. X., Pooley, D., et al. 2006, ApJ, 638, 354
- Cameron, P. B., & Frail, D. A. 2005, GRB Circular Network, 3676, 1
- Castro-Tirado, A. J., Gorosabel, J., de Ugarte Postigo, A., et al. 2005, GRB Circular Network, 3673, 1
- Champion, D. J., Lorimer, D. R., McLaughlin, M. A., et al. 2004, MNRAS, 350, L61
- Cobb, B. E., & Baily, C. D. 2005, GRB Circular Network, 3694, 1
- Cohen, E., & Piran, T. 1995, ApJ, 444, L25
- Covino, S., Malesani, D., Israel, G. L., et al. 2006, A&A, 447, L5
- Dezalay, J. P., Lestrade, J. P., Barat, C., et al. 1996, ApJ, 471, L27
- Eichler, D., Livio, M., Piran, T., & Schramm, D. 1989, Nature, 340, 126
- Fox, D. B. 2005, Nature, 437, 845
- Gal-Yam, A., Nakar, E., Ofek, E., et al. 2005a [arXiv:astro-ph/0509891]
- Gal-Yam, A., Cenko, S. B., Berger, E., Krzeminski, W., & Lee, B. 2005b, GRB Circular Network, 3681, 1

- Gandolfi, G., Smith, M. J. S., Coletta, A., et al. 2000, in *Gamma-Ray Bursts*, ed. R. M. Kippen, R. S. Mallozzi, & G. J. Fishman (New York: AIP), AIP Conf. Proc., 526, 23
- Gehrels, N., Sarazin, C. L., O'Brien, P. T., et al. 2005, *Nature*, 437, 851
- Guetta, D., Piran, T., & Waxman, E. 2005, *ApJ*, 619, 412 (GPW)
- Guetta, D., & Piran, T. 2005, *A&A*, 435, 421 (GP05)
- Hjort, J., Watson, D., Fynbo, J. P. U., et al. 2005, *Nature*, 437, 859
- Kalogera, V., Henninger, M., Ivanova, N., & King, A. R. 2004, *ApJ*, 603, L41, erratum, 2004, *ApJ*, 614, L137
- Katz, J. I., & Canel, M. 1996, *ApJ*, 471, 915
- Kouveliotou, C., Meegan, C. A., Fishman, G. J., et al. 1993, *ApJ*, 413, L101
- Kouveliotou, C., Koshut, T., Briggs, M. S., et al. 1996, in *Gamma-ray bursts*, Proc. of the 3rd Huntsville Symp., AIP Conf. Proc. Ser., 384, ed. Kouveliotou et al., 42
- Jensen, B. L., Jorgensen, U. G., Hjorth, J., et al. 2005, *GRB Circular Network*, 3589
- Mao, S., Narayan, R., & Piran, T. 1994, *ApJ*, 420, 171
- Narayan, R., Piran, T., & Kumar, P. 2001, *ApJ*, 557, 949
- Paciesas, W. S., Meegan, C. A., Pendleton, G. N., et al. 1999, *ApJS*, 122, 465
- Panaitescu, A., Kumar, P., & Narayan, R. 2001, *ApJ*, 561, L171
- Piran, T. 1992, *ApJ*, 389, L45
- Piran, T. 1994, *Gamma-Ray Bursts*, AIP Conf. Proc., 307 543 [arXiv:astro-ph/9412098]
- Porciani, C., & Madau, P. 2001, *ApJ*, 548, 522
- Price, P. A., Jensen, B. L., Jorgensen, U. G., et al. 2005, *GRB Circular Network*, 3612, 1
- Qin, Y.-P., Xie, G.-Z., Xue, S.-J., et al. 2000, *Publ. Astron. Soc. Japan*, 52, 759
- Romano, P., Moretti, A., Covino, S., et al. 2005, *GRB Circular Network*, 3669, 1
- Schmidt, M. 2001, *ApJ*, 559, L79
- Tanvir, N., Chapman, R., Levan, A. J., & Priddey, R. S. 2005, *Nature*, 438, 991
- Tavani, M. 1998, *ApJ*, 497, L21
- Villasenor, J. S., Lamb, D. Q., Ricker, G. R., et al. 2005, *Nature*, 437, 855
- Wiersema, K., Rol, E., Starling, R., et al. 2005, *GRB Circular Network*, 3699, 1